Habitable Planet, 2026, 2(1), 46–62

Scilight

Habitable Planet

Journal Homepage: https://www.sciltp.com/journals/hp

Review

Planetary Modulation of Solar and Climate Oscillations

Nicola Scafetta[1,*] and Antonio Bianchini[2]

[1] Department of Earth Sciences, Environment and Georesources, University of Naples Federico II, Complesso Universitario di Monte S. Angelo, via Cinthia, 21, 80126 Naples, Italy
[2] INAF – Astronomical Observatory of Padua, Vicolo Osservatorio 5, 35122 Padua, Italy
[*] Correspondence: nicola.scafetta@unina.it

ABSTRACT

Recent studies show that solar activity exhibits a complex array of oscillatory behaviors spanning from monthly to millennial scales. Among these, the 11-year Schwabe cycle stands out as the most widely recognized solar oscillation. A number of solar oscillations appear to influence Earth's climate and offer promising avenues for understanding and forecasting climate variability. The origin of this array of solar cycles is still debated within the scientific community. One prevailing view links solar cycles entirely to internal magnetic dynamo processes operating inside the Sun. An alternative hypothesis suggests that planetary gravitational interactions and orbital configurations may modulate the solar dynamo itself, introducing specific periodic solar oscillations. This study examines key observational findings that support the planetary hypothesis of the connection of solar variability with climate dynamics. It is shown that planetary-induced spectral features closely align with the dominant solar and climate cycles across a broad range of temporal scales.

ARTICLE INFO

History:

Received: 19 October 2025
Revised: 30 October 2025
Accepted: 7 November 2025
Published: 11 November 2025

Keywords:

Planetary systems;
Orbital synchronization;
Solar cycles;
Tidal forces;
Mechanisms of solar and climate cyclical variability

Citation:

Scafetta, N.; Bianchini, A. Planetary Modulation of Solar and Climate Oscillations. *Habitable Planet* **2026**, *2*(1), 46–62. https://doi.org/10.63335/j.hp.2025.0025

Research Highlights

- Planetary cycles may synchronize solar and climate oscillations over all timescales.
- Solar activity shows spectral coherences to planetary harmonics and tidal dynamics.
- Shared periodicities link solar variability to Holocene climate oscillations.
- Planetary-synchronized solar dynamo may improve climate model projections.

1. Introduction

Understanding how solar variability might affect the Earth's climate remains a central and unresolved question in climate science [1]. The challenge lies in the reliance on indirect proxies to reconstruct past solar activity and in the ongoing debate over the physical mechanisms that could mediate solar–climate interactions—whether through changes in solar irradiance or through

particle-based (corpuscular) influences. One promising line of inquiry focuses on identifying the drivers of solar variability and testing whether their signatures are observed in paleoclimatic records. Within this context, the so-called planetary hypothesis is emerging as a framework linking solar and climate variability with the solar system dynamics.

The notion that planetary alignments might modulate solar cycles dates to Wolf (1859) [2], who suggested that the frequency of sunspots could be influenced by the gravitational effects of Venus, Earth, Jupiter, and Saturn. Although this idea remained marginal throughout much of the 20th century [3–5], it has experienced a revival in the recent decades, accompanied by a growing body of literature that explores its possibility and implications [6]. Comprehensive reviews by Scafetta and Bianchini [7, 8] have synthesized this renewed interest, building on a series of earlier contributions by Scafetta.

The planetary hypothesis is not confined to explaining the 11-year Schwabe cycle. It also encompasses the entire range of solar periodicities, from intra-annual to multi-millennial scales. This extended framework has implications also for climate research, as multiple studies have reported spectral similarities between solar activity and climate proxies throughout the Holocene [9–13].

From a theoretical standpoint, two main paradigms have been proposed to explain the frequencies of the solar oscillations. One attributes all the variability to the internal processes of the solar dynamo. The other posits that planetary gravitational or tidal influences may partially synchronize the complex variability of solar activity. While the debate remains open—largely due to gaps in our understanding of solar physics—the possibility of external modulation remains a compelling hypothesis for further investigation, particularly considering its potential relevance for climate dynamics.

This perspective opens the door to new approaches for forecasting long-term solar and climate variability, drawing analogies with the harmonic models used in tidal prediction [14, 15]. Empirical studies have reinforced this view by showing that both solar and climate records exhibit spectral features consistent with planetary motions.

Detailed multi-proxy analysis of solar activity reveal strong correlations with climate indicators also during the 20th century [16]. Scafetta (2024) argued that empirically-based climate models that incorporate astronomical harmonics produce more physically reliable projections for the 21st-century warming [17]. Recent research further highlighted increasing uncertainties in climate attribution and modeling. This uncertainty could be reduced by including the presence of cyclical natural components, particularly those linked to solar and planetary dynamics [12].

In the following sections we examine the main evidences supporting the hypothesis that dominant solar and climate cycles may be synchronized with the principal planetary harmonics of the Solar System.

2. Evidence Supporting the Planetary Theory of Solar and Climate Variability

2.1. The Schwabe 11-year Solar Cycle and the Venus–Earth–Jupiter–Saturn Tidal System

Since the late 1800s, researchers have recognized that any credible connection between planetary dynamics and solar variability must consider the combined gravitational influence of several planets rather than isolated bodies. Although all planets exert some degree of tidal force on the Sun, Wolf [2] identified Venus, Earth, Jupiter, and Saturn as the smallest planetary group potentially capable of accounting for the 11-year solar cycle. Models that solely rely on a single planet—even Jupiter—are inadequate. In fact, while Jupiter's orbital period of 11.86 years is numerically close to the Schwabe cycle, its tidal phase alignment does not consistently match the timing of the Schwabe sunspot cycle, whose period is on average 11 years.

Wolf's hypothesis was based on a comparative ranking of planetary tidal strengths, ordered from the strongest to the weakest: Jupiter, Venus, Earth, Mercury, Saturn, Mars, Uranus, and Neptune [14]. Due to Mercury's rapid revolution and the relatively weak tidal effects of Mars, Uranus, and Neptune, these four planets were considered less relevant. As a result, the Venus–Earth–Jupiter–Saturn configuration emerged as a physically plausible one. Some researchers even focused on the Venus–Earth–Jupiter triad, which dominates the tidal signal, although this simplification does neglect important dynamical contributions captured by a complementary model based on Jupiter and Saturn [11].

The concept of a Venus–Earth–Jupiter tidal alignment influencing solar variability dates back over a century [3, 4, 18] and has since evolved through more sophisticated modeling in recent decades [14, 19–26]. These models generally propose that when Jupiter and Venus align with Earth and the Sun—either in conjunction or opposition—their combined tidal forces may exert a stronger influence on the solar internal dynamics. Indeed, their resulting tidal beats exhibit a strong correlation with the 11-year sunspot cycle observed from 1700 to the present (see Figure 1). The dominant periodicity associated with them can be derived from their orbital parameters, yielding a value close to 11.07 years:

$$P_{VEJ} = \frac{1}{2}\left(\frac{3}{P_V} - \frac{5}{P_E} + \frac{2}{P_J}\right)^{-1} = 11.07 \text{ year} \quad (1)$$

where $P_V = 224.701$ days, $P_E = 365.256$ days, and $P_J = 4332.589$ days are the sidereal orbital periods of Venus, Earth, and Jupiter, respectively [14]. This periodicity can also be reformulated as:

$$P_{VEJ} = \frac{1}{2}\left[3\left(\frac{1}{P_V} - \frac{1}{P_E}\right) - 2\left(\frac{1}{P_E} - \frac{1}{P_J}\right)\right]^{-1} = \left[\frac{1}{2P_{VE}} + \left(\frac{1}{P_{VE}} - \frac{1}{P_{EJ}}\right)\right]^{-1} = 11.07 \text{ year} \quad (2)$$

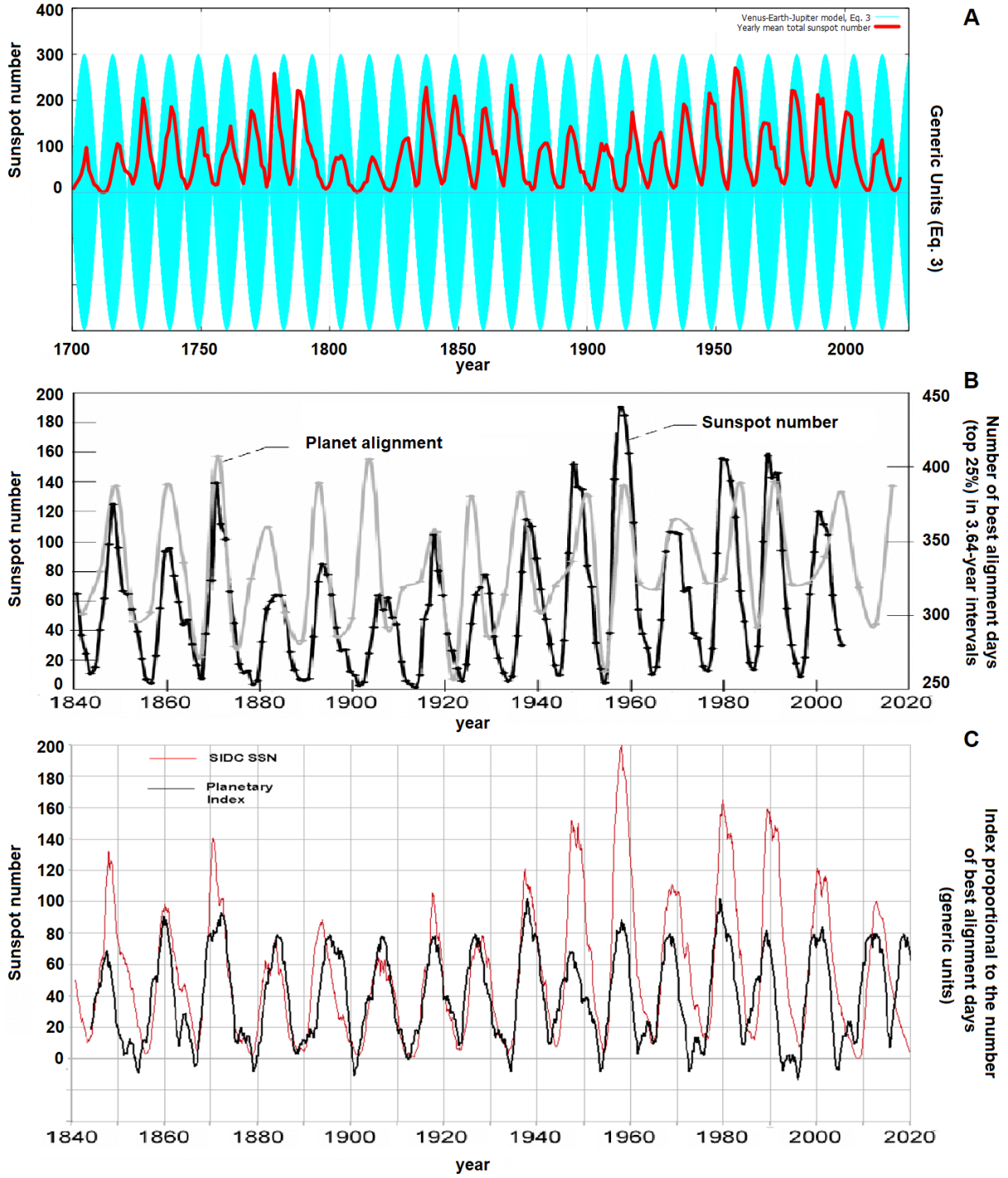

Figure 1. (**A**) Diagrammatic comparison between the Venus–Earth–Jupiter harmonic model and the annual sunspot count from 1700 to 2021, as derived from Equation (3). (**B**) Planetary alignment configuration as proposed by [19]. (**C**) Planetary alignment scheme according to Ref. [21]. (From Ref. [8].)

which reveals important mathematical properties. In fact, P_{VEJ} represents a beat period between the third harmonic of the Venus–Earth synodic cycle (P_{VE} *being* $(1/P_V - 1/P_E)^{-1} = 1.59867$ years) and the second harmonic of the Earth–Jupiter synodic cycle ($P_{EJ} = (1/P_E - 1/P_J)^{-1} = 1.09207$ years). The factor $\frac{1}{2}$ converts synodic periods into spring tidal cycles. Thus, Equation (2) can also be interpreted as the beat period between the second upper harmonic of the Venus–Earth synodic cycle (P_{VE}) and the beat interaction between the synodic cycles of the pairs Venus–Earth ($P_{VE} = 0.799$ year) and Earth–Jupiter ($P_{EJ} = 0.546$ year).

Table 1 provides the orbital parameters of each planet, while Table 2 reports the spring tidal periods associated with all possible planetary pairs. By combining these frequencies, one can reconstruct the full spectrum of the

Table 1. The planetary orbital data. From https://nssdc.gsfc.nasa.gov/planetary/factsheet/. (Adapted from Refs. [8].)

	Mass m_P (kg)	Sidereal orbital period T_P (day)	Semimajor axis d_P (m)	Aphelion d_a (m)	Aphelion date t_a	Angular separation $\alpha_{J,2000}$ (deg)
Mercury	3.301000E ± 23	87.969	5.790900E ± 10	6.981800E ± 10	2000.0047	143.6
Venus	4.867300E ± 24	224.701	1.082100E ± 11	1.089410E ± 11	2000.2219	145.5
Earth	5.972200E ± 24	365.256	1.495980E ± 11	1.521000E ± 11	2000.5087	63.6
Mars	6.416900E ± 23	686.98	2.279560E ± 11	2.492610E ± 11	2000.8405	37.1
Jupiter	1.898130E ± 27	4332.589	7.784790E ± 11	8.163630E ± 11	2005.2841	0.0
Saturn	5.683200E ± 26	10759.22	1.432041E ± 12	1.506527E ± 12	1988.6954	9.5
Uranus	8.681100E ± 25	30685.4	2.867043E ± 12	3.001390E ± 12	2009.1554	79.8
Neptune	1.024090E ± 26	60189	4.514953E ± 12	4.558857E ± 12	1959.5619	92.3

Table 2. Spring tidal periods, $P_{12} = 0.5/|1/P_1 - 1/P_2|$, of pairs of the planets in days and in years. The most relevant ones are in bold. (Adapted from Refs. [8].)

(days)	Mercury	Venus	Earth	Mars	Jupiter	Saturn	Uranus	Neptune
Mercury		**72.3**	57.9	50.4	44.9	44.3	44.1	44.0
Venus	**72.3**		**292.0**	167.0	**118.5**	114.7	113.2	112.8
Earth	57.9	**292.0**		390.0	**199.4**	189.0	184.8	183.7
Mars	50.4	167.0	390.0		408.2	366.9	351.4	347.5
Jupiter	44.9	**118.5**	**199.4**	408.2		**3626.7**	2522.4	2334.3
Saturn	44.3	114.7	189.0	366.9	**3626.7**		8284.4	6550.6
Uranus	44.1	113.2	184.8	351.4	2522.4	8284.4		31300.0
Neptune	44.0	112.8	183.7	347.5	2334.3	6550.6	31300.0	
(years)	Mercury	Venus	Earth	Mars	Jupiter	Saturn	Uranus	Neptune
Mercury		**0.198**	0.159	0.138	0.123	0.121	0.121	0.121
Venus	**0.198**		**0.799**	0.457	**0.324**	**0.314**	0.310	0.309
Earth	0.159	**0.799**		1.07	**0.546**	0.518	0.506	0.503
Mars	0.138	0.457	1.07		1.12	1.00	0.962	0.951
Jupiter	0.123	**0.324**	**0.546**	1.12		**9.93**	6.91	6.39
Saturn	0.121	**0.314**	0.518	1.00	**9.93**		22.7	17.9
Uranus	0.121	0.310	0.506	0.962	6.91	22.7		85.7
Neptune	0.121	0.309	0.503	0.951	6.39	17.9	85.7	

planetary harmonics [27, 28]. Equation (1) illustrates a particular class of harmonic relationships referred to as orbital commensurabilities with invariant properties, which are explored in detail in Section 2.3. That section shows that these orbital frequencies remain stable also when analyzed across different rotating reference frames [27]. Such an invariance may play a key role in enabling synchronization processes within the solar dynamo, which itself is governed by Sun's differential rotation.

The tidal beat described by Equation (1) can be written as:

$$f(t) = \cos\left(2\pi \cdot 3\frac{t - t_{VE}}{P_{VE}}\right) + \cos\left(2\pi \cdot 2\frac{t - t_{EJ}}{P_{EJ}}\right), \quad (3)$$

where $t_{VE} = 2002.8327$ corresponds to a Venus–Earth conjunction epoch, and $t_{EJ} = 2003.0887$ an Earth–Jupiter conjunction. Each cosine term represents the spring tidal maxima associated with the respective planetary alignments. Thus, Equation (3) is entirely constructed from astronomical parameters.

Figure 1A presents a comparison between the output of Equation (3) (in cyan) and the annual sunspot number series (in red) spanning the years from 1700 to 2021. Although the model does not simulate low-frequency components, it clearly highlights a dominant oscillation near 11.07 years that closely aligns with the observed sunspot cycle. This coherence suggests that the periods of increased sunspot activity may coincide with more frequent alignments among Venus, Earth, and Jupiter, potentially amplifying the tidal forcing at the solar tachocline, thus modulating the solar magnetic field generation.

Figures 1B and 1C provide further evidence that different formulations of the Venus–Earth–Jupiter syzygy model successfully replicate both the solar cycle timing and periodicity over several centuries [19, 21]. Subsequent sections explore how these models can be extended to account for longer-term modulations. Additionally, if the ½ factor in Equation (1) is omitted, the resulting dominant period becomes 22.14 years—matching the average duration of the Hale solar magnetic cycle [20].

To properly generalize the tidal signal that can be generated by all the planets, one may adopt the following simplified yet physically motivated tidal function:

$$Tide(t) = \sum_P \frac{m_P}{[d_P + (d_{Pa} - d_P)\cos(2\pi \frac{t - t_{Pa}}{\frac{T_P}{365.25}})]^3} \cdot \left[\cos^2\left(2\pi \frac{t-2000}{\frac{T_S}{365.25}} - 2\pi \frac{t-2000}{\frac{T_P}{365.25}} - 2\pi \frac{\alpha_{PJ,2000}}{360^\circ}\right) - \frac{1}{3}\right], \quad (4)$$

where d_P is the average heliocentric distance of planet P, m_P its mass, $T_S = 27.3$ days the solar rotation period, and T_P the orbital period of planet P. The parameters d_{Pa} and t_{Pa} denote the aphelion distance and its epoch, respectively, while $\alpha_{PJ,2000}$ is the angular separation relative to the Sun between planet P and Jupiter on January 1, 2000.

The physically relevant quantity of interest is the tidal power dissipated within the Sun, which corresponds to the rate of work done by tidal forces [14]. This can be approximated by:

$$f(t) \propto \left|\frac{dTide(t)}{dt}\right| \approx \left|\frac{Tide(t) - Tide(t - 1\ \text{day})}{1\ \text{day}}\right|. \quad (5)$$

Equation (5) can be interpreted as a proxy of the instantaneous rate of the tidal energy dissipated within the solar core. The portion of this energy absorbed in the solar core could potentially influence the radiative output. To model this effect more accurately, Scafetta [14] introduced a refined tidal function—an improvement of Equation (4)—designed to estimate the theoretical luminosity variations induced by planetary tides in the solar core.

Figure 2A displays the evolution of the function $f(t)$ (Equation (5)) when restricted to the gravitational

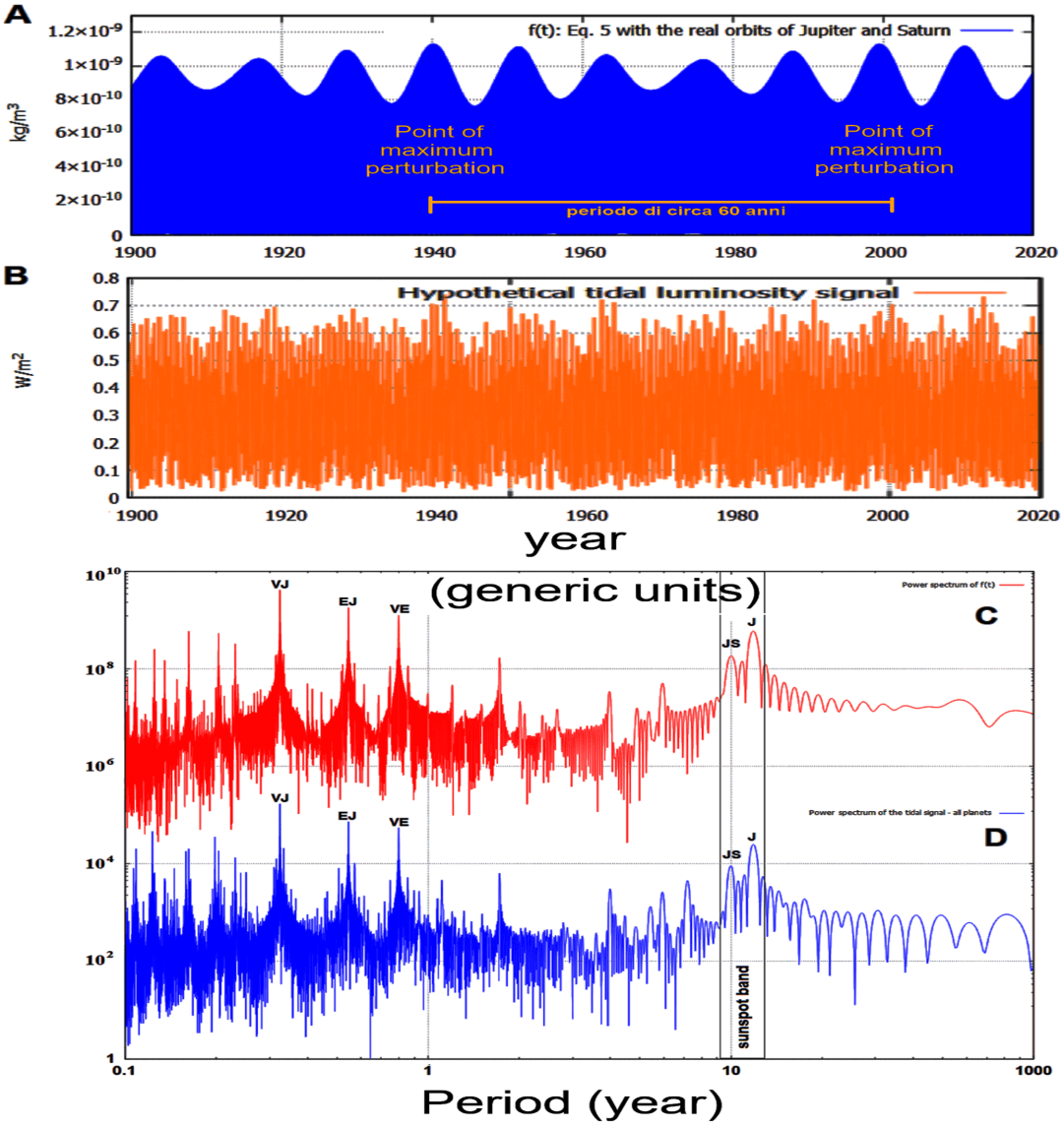

Figure 2. (**A**) Output of Equation (5), $f(t)$, assuming elliptical orbital paths for Jupiter and Saturn. (**B**) Hypothetical luminosity variation induced by planetary tides, calculated following [11]. (**C**–**D**) Spectral analysis of the tidal function $f(t)$ and of the tidal-induced luminosity signal using all planetary bodies. (From Ref. [8].)

contributions of Jupiter and Saturn. The resulting signal reveals a quasi-periodic pattern with a dominant cycle of approximately 11.86 years, which coincides with Jupiter's orbital period. This primary oscillation is further modulated by a secondary 9.93-year cycle, which arises from the spring tidal interaction between Jupiter and Saturn. Together, these two periodicities constrain an 11-year periodicity which closely matches the canonical Schwabe 11-year-sunspot cycle. Figure 2A shows that these tidal effects were particularly pronounced around 1940 and 2000—periods that also correspond to multi-decadal peaks observed in global surface temperature records [29].

Figure 2B presents the hypothetical variation of the solar luminosity resulting from the combined tidal forces of all the planets [14]. Figures 2C and 2D compare the frequency spectral of the tidal function $f(t)$, derived from the Venus–Earth–Jupiter–Saturn configuration, with that of the luminosity function generated in the solar core by the whole planetary system (Figure 2B). Both spectra exhibit multiple harmonic features, most of which are linked to planetary spring tides. Two particularly strong spectral peaks appear in the 9–13-year band, corresponding to the 9.93-year Jupiter–Saturn-spring tide and the 11.86-year orbital period of Jupiter. These two frequencies cover the spectral domain of the Schwabe sunspot cycle, emphasizing the importance of incorporating precise orbital data when investigating the planetary modulation of solar activity.

One of the central findings is that the Schwabe cycle does not represent a single-frequency oscillation but rather emerges from the interference of multiple harmonics. In particular, the presence of components near 10 and 12 years suggests that the observed 11-year solar cycle might well result from a synchronization process occurring in the solar dynamo—producing a primary oscillation near 11 years—and two secondary harmonics at 9.93 and 11.86 years, associated with the Jupiter–Saturn spring tide (P_{SJ}) and Jupiter's orbital period (P_J), respectively. This triplet frequency beat is clearly visible in Figure 3, which shows periodograms of sunspot records with three peaks in the 10–12-year range. The same configuration has been independently identified by other researchers [30], reinforcing the hypothesis that planetary dynamics may play a role in shaping solar variability.

In summary, five key tidal harmonics generated by Venus, Earth, Jupiter, and Saturn—namely P_{VJ}, P_{EJ}, P_{VE}, P_{SJ}, and P_J—appear to collectively reconstruct the

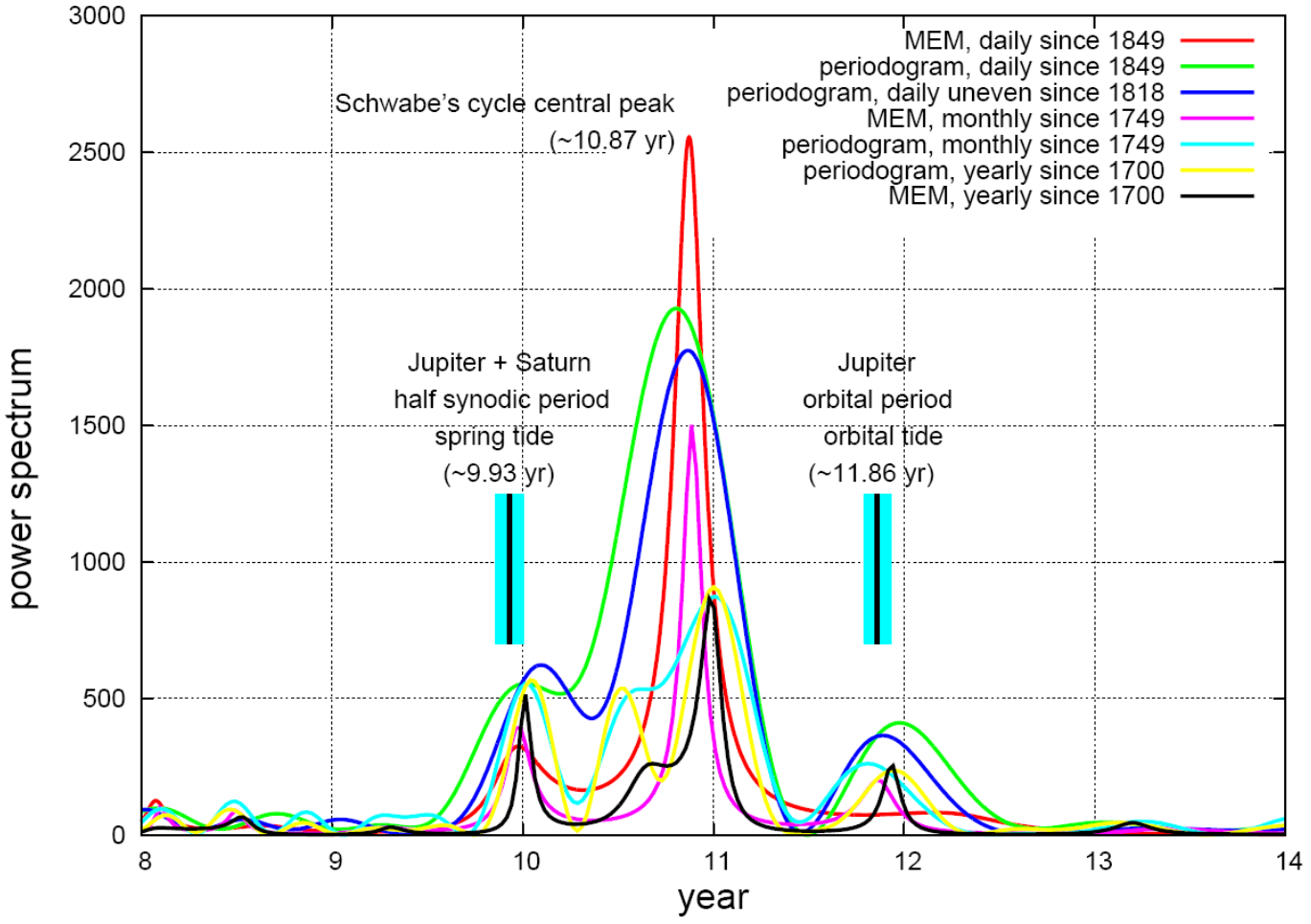

Figure 3. Spectral decomposition of the sunspot-number record across different time intervals and resolutions. (From Ref. [8].)

Schwabe 11-year sunspot cycle. This outcome supports to the hypothesis originally advanced by Wolf [2].

2.2. Multi-decadal to Millennial Timescales

Beyond the well-known 11-year Schwabe cycle, numerous studies have documented that solar variability—reconstructed through cosmogenic proxies such as ^{14}C and ^{10}Be isotopes generated by cosmic ray particles colliding with the atmosphere molecules—manifests a wide spectrum of periodicities, ranging from decadal to millennial time scales. These cycles tend to cluster within specific frequency bands, including approximately 40–45 years, 55–65 years, 80–105 years (commonly referred to as the Gleissberg cycle), 115–150 years, 170–240 years (associated with the Jose and Suess–de Vries cycles), 800–1200 years (Eddy cycle), and 2000–2500 years (Bray–Hallstatt cycle) [1, 9, 10, 31–34].

A growing body of research has shown that these solar oscillations closely correspond to harmonic structures derived from planetary orbital configurations [34–37]. The following section outlines the principal findings emerging from this line of investigation.

Herein we summarize the main findings by Scafetta [11], who proposed a harmonic model of solar and climate variability structured around three key periodic drivers: the spring tidal interaction between Jupiter and Saturn, the orbital tidal cycle of Jupiter, and a hypothesized fundamental oscillation of the solar dynamo with a period of approximately 10.87 years. The interplay among these three frequencies gives rise to four principal beat cycles: 60.95, 114.78, 129.95, and 983 years. These longer-term modulations align well with the timing of the major solar minima observed over the last millennium, including the Oort, Wolf, Spörer, Maunder, and Dalton episodes (Figure 4A). The same model also reproduces multi-decadal and millennial-scale climate oscillations—specifically those in the 115–130-year and ∼1000-year ranges—found in Northern Hemisphere temperature reconstructions spanning the past two thousand years (Figure 4B). When compared with global surface temperature records since 1850, the model reveals a ∼60-year oscillation superimposed to a longer millennial warming oscillation (Figure 4C).

Extending the analysis to the Holocene, the quasi-millennial beat cycle derived from this planetary framework successfully reconstructs the timing of solar and climatic fluctuations over the past 10,000 years. Figure 5A shows the agreement between the millennial component of the model and the total solar irradiance (TSI) proxy reconstruction [32], while Figure 5B shows a similar pattern in summer temperature reconstructions for the European Alps [38]. Figure 5C confirms the same oscillatory behavior in summer air temperature data from the Greenland Ice Sheet, based on GISP2 ice core records [39].

In a follow-up study, the same three-frequency model also produces additional harmonic sets which are typically observed in solar cosmogenic and climate records [15]: one centered around 57, 61, and 65 years, and another spanning 103, 115, 130, and 150 years. These extended cycles are associated with the emergence of grand solar minima and maxima and have been identified in solar activity datasets reaching back as far as 340,000 to 320,000 years. The findings presented above directly challenge the conclusions drawn by Cauquoin et al. [40], who argued that there is no compelling evidence supporting a planetary origin for solar variability. They also refute the claim made by Smythe and Eddy [41], who dismissed the possibility that tidal models involving planetary alignments could explain episodes such as the Maunder Minimum. Furthermore, these results respond to the criticisms raised by some other authors [42]—already addressed in detail in Ref. [43]—who suggested that solar fluctuations beyond the 11-year Schwabe cycle might arise from random or stochastic processes rather than structured astronomical influences.

2.3. The Orbital Invariant Inequality Model of Solar and Climate Oscillations

Long-term solar variability—from multi-decadal to millennial time scales—exhibits spectral coherence with a specific class of planetary harmonics referred to as "*orbital invariant inequalities*" [27, 37]. These harmonics emerge from beat interactions among synodic cycles of planetary pairs as observed from the Sun. In systems characterized by differential rotation, such as the solar convective zone, these periodicities retain mathematical invariance with respect to any rotating frame of reference, a property that may enable phase-locking mechanisms between planetary dynamics and the magnetic activity originating in the solar convective zone.

Ref. [27] further identified that the orbital invariant inequalities generated by the outer planets—Jupiter, Saturn, Uranus, and Neptune—produce distinct clusters of periodicities within the following ranges: 42–47 years, 55–65 years, 80–105 years (associated with the Gleissberg cycle), 160–185 years (Jose cycle), 200–240 years (Suess–de Vries cycle), 770–1160 years (Eddy cycle), and 2000–2500 years (Bray–Hallstatt cycle). These groupings encompass all major known secular and millennial solar and climate cycles, suggesting that the long-term modulation of solar activity may be largely governed by the gravitational architecture of the Jovian planets.

The mathematical framework underlying these orbital inequalities employs vector notation to represent synodic interactions. For example, the vector $(1, -1)$ corresponds to the synodic period T_{12} between two planets with orbital periods T_1 and T_2, calculated as $T_{12} = (1/T_1 - 1/T_2)^{-1}$. More complex inequalities are derived by linear combinations of such synodic vectors across multiple planetary pairs. Table 1 summarizes the orbital periods of the planets, while Table 2 lists the spring tidal periods—defined as half the synodic period—for each pair.

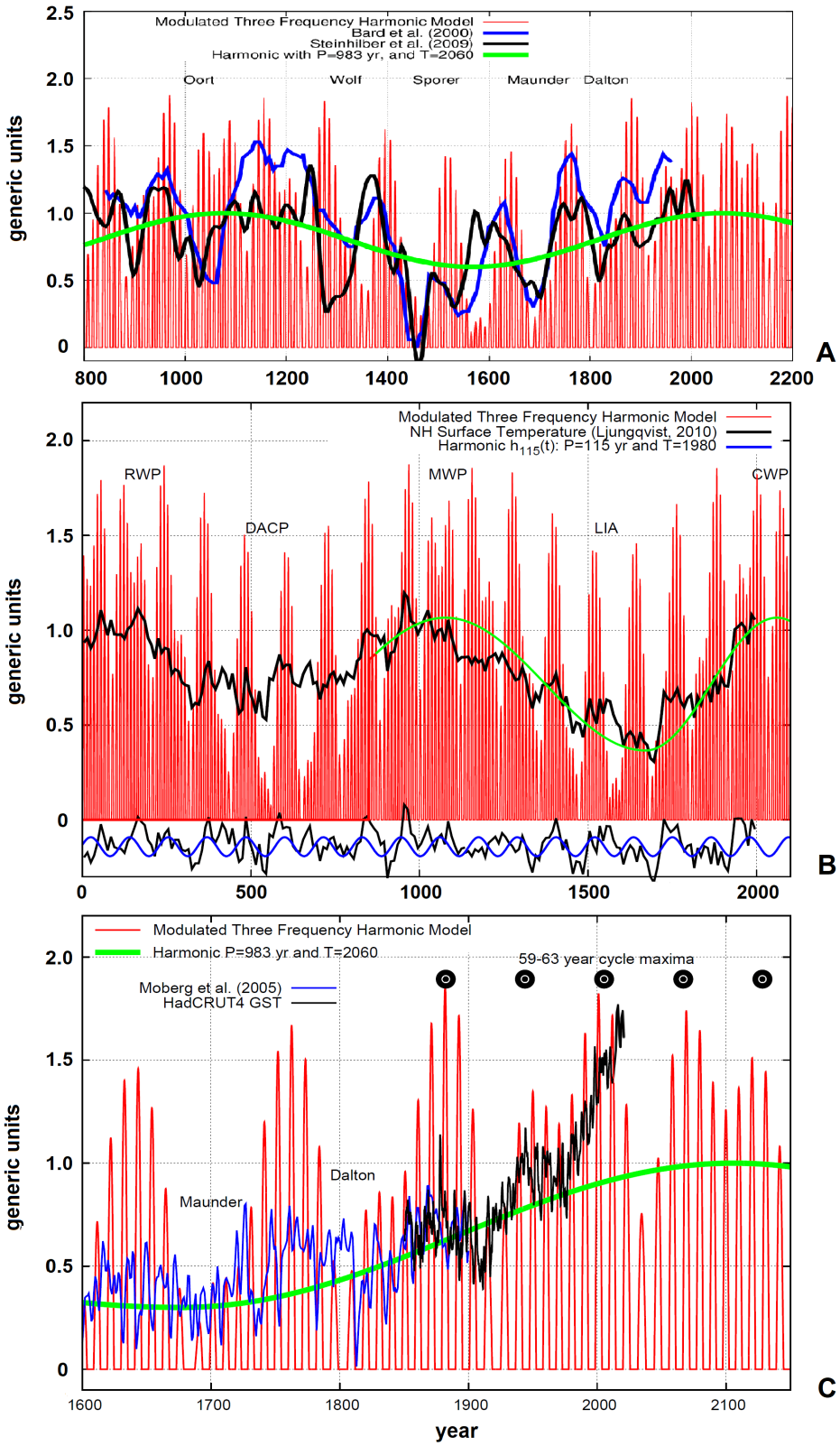

Figure 4. (**A**) Comparison between the three-frequency Jupiter–Saturn model (red) and two solar activity reconstructions based on ^{10}Be and ^{14}C isotopes [13, 44]. (**B**) Superposition of the same solar model (red) on a Northern Hemisphere temperature reconstruction (black) from Ref. [45]; the insert compares long-term solar modulation (blue) with corresponding climate variability (black). (**C**) Comparison between the planetary model (red) and global temperature records from 1600 to 2010 [46], highlighting cold phases during the Maunder and Dalton minima and a repeating 60-year cycle since 1880. (From Ref. [8].)

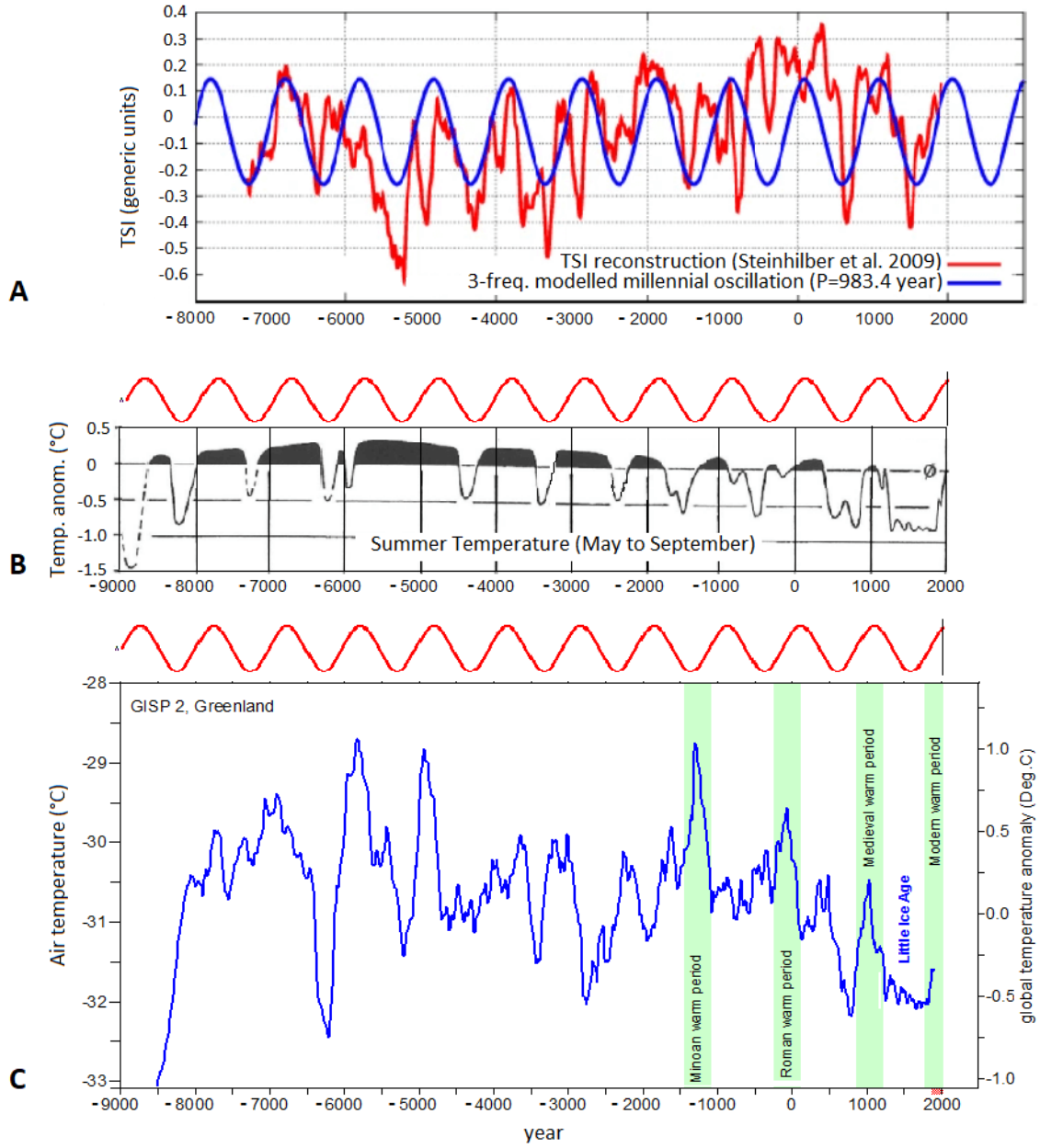

Figure 5. (**A**) Overlay of the planetary model's millennial component (blue) with the solar proxy reconstruction by [32] (red). (**B**) Comparison between the quasi-millennial oscillation of the planetary model (red) and summer temperature reconstructions in the European Alps (black), based on glacier and tree-line proxies [38]. (**C**) Reconstructed summit temperatures of the Greenland Ice Sheet from GISP2 ice core data [39]. (From Ref. [8].)

In general, the periodicity of an orbital commensurability among N planets with orbital periods equal to $T_1, \ldots, T_N$ is defined as

$$f = \frac{1}{T} = \left| \sum_{i=1}^{n} \frac{a_i}{T_i} \right|, \tag{6}$$

with $(a_1, \ldots, a_n)$ being a vector of integer numbers. This frequency is defined as an "*orbital invariant inequality*" if

$$\sum_{i=1}^{n} a_i = 0. \tag{7}$$

For example, assuming only the four Jovian planets and that Jupiter's orbital frequency $(f_J = 1/T_J)$ is represented as the vector (1, 0, 0, 0), Saturn's orbital frequency $(f_S = 1/T_S)$ as (0, 1, 0, 0), Uranus' orbital frequency $(f_U = 1/T_U)$ as (0, 0, 1, 0) and Neptune's orbital frequency $(f_U = 1/T_N)$ as (0, 0, 0, 1), the frequency of the synodic cycle between Jupiter and Saturn can be written as

$$f_{SJ} = f_J - f_S = (1, 0, 0, 0) - (0, 1, 0, 0) = (1, -1, 0, 0). \tag{8}$$

Accordingly, that of Jupiter and Uranus as (1, 0, −1, 0), that of Jupiter and Neptune as (1, 0, 0, −1), and so on

for the other pairs of planets. The synodic periodicities and all their linear combinations are orbital invariant inequalities because the sum of their coefficients is zero.

Following such this formalism, all the beats among the planetary synodic cycles can be obtained by linearly combining them. For example, the longest oscillation identified in the Holocene in both solar and climate records is the Bray–Hallstatt oscillation of about 2100–2500 years, which can be predicted by the vector

$$(1, -3,\ 1,\ 1) = (1, -1,\ 0,\ 0) - (0,\ 1,\ -1,\ 0) - (0,\ 1,\ 0,\ -1), \quad (9)$$

that represents the orbital invariant inequality generated by the synodic cycles between Jupiter and Saturn $(1, -1,\ 0,\ 0)$, Saturn and Uranus $(0,\ 1,\ -1,\ 0)$ and Saturn and Neptune $(0,\ 1,\ 0,\ -1)$.

Using the orbital periods of Jupiter, Saturn, Uranus and Neptune listed in Table 1, the orbital invariant inequality (1, −3, 1, 1) has period

$$T_{(1,-3,1,1)} = (1/T_J - 3/T_S + 1/T_U + 1/T_N)^{-1} = 2318 \text{ years}. \quad (10)$$

Table 3, adapted from Ref. [28], presents the principal orbital invariant inequalities generated by the outer planets—Jupiter, Saturn, Uranus, and Neptune—and their additional beat interactions with Jupiter's orbital period. These harmonics are among the most influent ones in shaping the gravitational oscillations that govern both the

Table 3. Complete list of orbital invariant inequalities with periods $P \geq 40$ years. Column 2 reports the maximum absolute value of the integer coefficients a_i (with $M < 6$), while column 3 indicates the number K of synodic terms involved in each relation. Columns 5 and 6 present the beat interactions between each inequality vector (a_1, a_2, a_3, a_4) and Jupiter's orbital frequency, represented by the vector (1, 0, 0, 0), yielding the transformed vector $(a_1 - 1, a_2, a_3, a_4)$. (Adapted from Ref. [28].)

				Their beats with Jupiter	
(Jup, Sat, Ura, Nep)	(M, K)	P_{model} (year)	Cluster	(Jup −1, Sat, Ura, Nep)	P_{model} (year)
(1,−3,5,−3)	(5, 6)	42.069 ± 0.002		***(0−1,3,−2,−1)***	81.072 ± 0.004
(0,0,4,−4)	(4, 4)	42.847 ± 0.002		***(2−1,−3,4,−3)***	84.265 ± 0.007
(2,−5,1,2)	(5, 5)	43.653 ± 0.002		***(2−1,−3,0,1)***	87.171 ± 0.004
(1,−3,−3,5)	(5, 6)	43.654 ± 0.002	∼***45*** yr	***(1−1,0,3,−4)***	87.445 ± 0.005
(1,−2,0,1)	(2, 2)	44.591 ± 0.001		***(0−1,2,3,−5)***	90.575 ± 0.006
(0,1,−1,0)	(1, 1)	45.362 ± 0.001		***(3−1,−5,0,2)***	90.870 ± 0.007
(1,−4,2,1)	(4, 4)	46.268 ± 0.002		***(0−1,3,2,−5)***	90.873 ± 0.006
(1,−1,−5,5)	(5, 6)	47.209 ± 0.002		***(1−1,−1,4,−4)***	94.259 ± 0.007
(1,−3,4,−2)	(4, 5)	55.754 ± 0.003		***(2−1,−2,−1,1)***	94.579 ± 0.004
(0,0,3,−3)	(3, 3)	57.129 ± 0.003		***(2−1,−4,5,−3)***	98.25 ± 0.01
(2,−5,0,3)	(5, 5)	58.571 ± 0.003		***(1−1,1,−2,0)***	98.603 ± 0.004
(1,−3,−2,4)	(4, 5)	58.573 ± 0.003	∼***60*** yr	***(0−1,4,−3,−1)***	102.98 ± 0.01
(1,−2,−1,2)	(2, 3)	60.090 ± 0.003		***(1−1,1,−5,3)***	135.82 ± 0.02
(0,1,−2,1)	(2, 2)	61.690 ± 0.003		***(2−1,−2,−4,4)***	144.28 ± 0.02
(1,−4,3,0)	(4, 4)	63.377 ± 0.004		***(0−1,3,−1,−2)***	153.85 ± 0.02
(1,−3,3,−1)	(3, 4)	82.638 ± 0.005		***(3−1,−5,−3,5)***	153.86 ± 0.03
(0,0,2,−2)	(2, 2)	85.693 ± 0.005		***(2−1,−3,3,−2)***	165.77 ± 0.02
(2,−5,−1,4)	(5, 6)	88.981 ± 0.007		***(2−1,−3,1,0)***	177.40 ± 0.02
(1,−3,−1,3)	(3, 4)	88.984 ± 0.005	Gleissberg	***(1−1,0,2,−3)***	178.54 ± 0.02
(1,−2,−2,3)	(3, 4)	92.533 ± 0.005		***(3−1,−5,−1,3)***	193.43 ± 0.04
(0,1,−3,2)	(3, 3)	96.382 ± 0.006		***(0−1,3,1,−4)***	193.44 ± 0.02
(1,−4,4,−1)	(4, 5)	100.56 ± 0.01		***(1−1,−1,5,−5)***	209.45 ± 0.05
(1,−3,2,0)	(3, 3)	159.585 ± 0.02		***(2−1,−2,−2,2)***	211.04 ± 0.02
(0,0,1,−1)	(1, 1)	171.39 ± 0.01	Jose	***(1−1,1,−3,1)***	232.18 ± 0.04
(2,−5,−2,5)	(5, 7)	185.06 ± 0.03		***(0−1,4,−4,0)***	258.04 ± 0.07
(1,−3,0,2)	(3, 3)	185.07 ± 0.02		***(0−1,4,−5,1)***	510.4 ± 0.3
(1,−2,−3,4)	(4, 5)	201.12 ± 0.03		***(1−1,1,−4,2)***	654.5 ± 0.4
(0,1,−4,3)	(4, 4)	220.23 ± 0.04	Suess-de Vries	***(2−1,−2,−3,3)***	912.1 ± 0.6
(1,−4,5,−2)	(5, 6)	243.36 ± 0.07		***(0−1,3,0,−3)***	1503 ± 2
(0,1,−5,4)	(5, 5)	772.7 ± 0.6	Eddy	***(3−1,−5,−2,4)***	1504 ± 2
(1,−2,−4,5)	(5, 6)	1159 ± 2		***(1−1,0,1,−2)***	4279 ± 4
(1,−3,1,1)	(3, 3)	2318 ± 3	Bray–Hallstatt	***(2−1,−3,2,−1)***	5056 ± 16

solar inertial motion and the dynamics of the heliosphere [37].

Nonetheless, similar invariant periodicities can be constructed using inner planets or mixed configurations involving both terrestrial and Jovian bodies. For instance, Equation (1) represents the fundamental harmonic—equivalent to a spring tidal cycle—of an invariant inequality involving Venus, Earth, and Jupiter. This is evident from its structural equivalence to Equation (6), where the sum of the integer coefficients equals zero: $2 - 5 + 3 = 0$.

Figure 6 synthesizes the key results. Panel 6A compares a solar proxy (Δ^{14}C) with a climate proxy (δ^{18}O) over the interval 9500–6000 years before present, revealing a strong spectral alignment between the two datasets [9]. Panel 6B superimposes the orbital invariant inequalities of the solar system (red bars, from Table 3) onto the cross-spectral peaks identified in panel 6A, showing that the planetary harmonics coincide with the shared frequencies of both solar and climate variability. Panel 6C illustrates the oscillation produced by the $(1, -3, 1, 1)$ invariant inequality (blue curve), whose phase is computed solely from astronomical parameters [27, 37], and is found consistent with the Δ^{14}C record [47]. The result demonstrates a strong correspondence of the calculate harmonic cycle with the Bray–Hallstatt cycle found in the data.

The Bray–Hallstatt cycle, with a periodicity between 2000 and 2500 years, is consistently observed in solar activity reconstructions [33, 34, 48] and in paleoclimatic archives [37, 49, 50]. Notable climatic downturns such as the Greek Dark Ages (1000–550 B.C.) and the Little Ice Age (1350–1850 A.D.) are well-documented episodes that coincide with the grand solar minima linked to this long cycle, as shown in Figure 6C. The Bray–Hallstatt cycle also provides a framework for interpreting Holocene climate

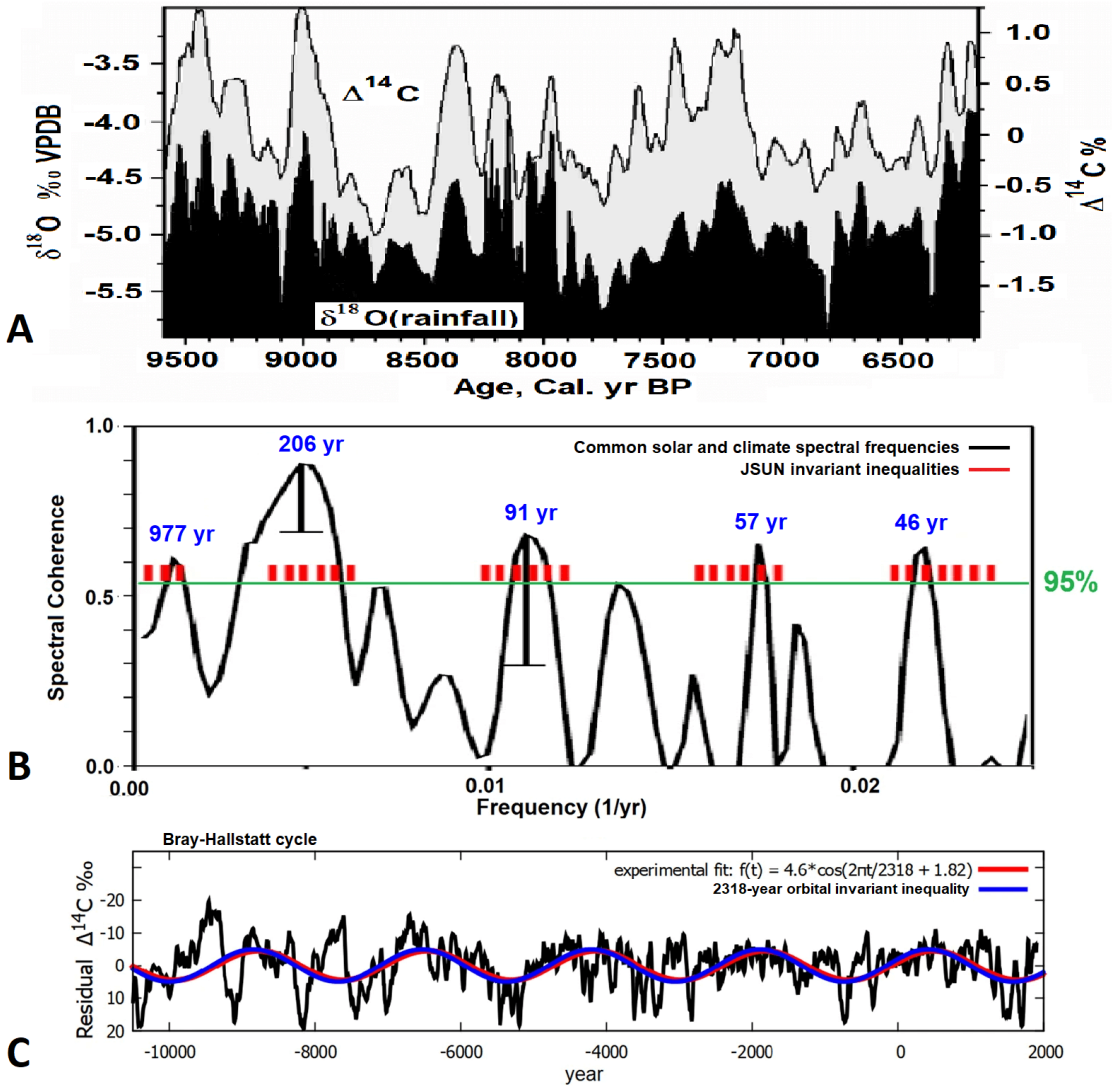

Figure 6. (**A**) Comparative analysis of solar (Δ^{14}C) and climate (δ^{18}O) records between 9500 and 6000 years BP, adapted from [9]. (**B**) Cross-spectral peaks between the records in panel A (black) compared with orbital invariant inequalities of the solar system (red bars), as calculated in Ref. [27]. (**C**) Overlay of the 2318-year Bray–Hallstatt oscillation (blue) with the residuals of the Δ^{14}C record (black and red) from Ref. [47]. (From Ref. [8].)

phases based on palynological and stratigraphic records, particularly from Northern Europe. These include: the Preboreal (11,700–10,000 cal BP), marking the onset of postglacial warming; the Boreal (10,000–9,000 cal BP), characterized by forest expansion; the Atlantic (9,000–5,000 cal BP), corresponding to the Holocene Thermal Maximum; the Subboreal (5,000–2,500 cal BP), indicating gradual cooling; and the Subatlantic (2,500 cal BP to present), marked by increased climatic variability and events such as the Medieval Warm Period and the Little Ice Age. LIA—the coldest interval of the Holocene—is explained by the overlapping minima of both the millennial Eddy cycle and the Bray–Hallstatt cycle [12].

Ultimately, the harmonic structures derived from the orbital invariant inequality model, as recently refined in Ref. [28], successfully reproduce all known frequencies associated with the solar inertial motion documented in the literature [51–53].

2.4. Additional Empirical Indications of a Planetary Modulation of Solar Activity

There are different sets of empirical findings that reinforce the plausibility of a planetary influence on solar activity. For example, Hung (2007) observed that 25 of the 38 most powerful solar flares occurred when Mercury, Venus, Earth, or Jupiter were either aligned above the flare site (within 10° longitude) or positioned directly opposite on the solar disk [19]. Related discussions on planetary alignments and solar phenomena have been discussed in other works [54, 55]. Additional evidence of planetary harmonics has emerged in studies of auroral patterns and long-term climate variability [15, 56].

Fluctuations in the Sun's angular momentum—primarily influenced by Uranus and Neptune—correlate with peaks in ^{14}C and ^{10}Be solar proxy records throughout the Holocene [57]. Cosmic ray intensity tends to diminish during superior conjunctions of Uranus and Neptune, and intensify during inferior ones, implying a modulation of the Sun's magnetic shielding capacity over extended timescales [34]. The synodic cycle of Uranus and Neptune, repeating every 171.4 years, aligns with the Jose frequency band reported in Table 3.

A strong spectral coherence is found between long-term solar activity proxies and the torque exerted by planetary configurations on a hypothesized non-spherical tachocline at the base of the solar convection zone [58]. Some of these periodicities remained phase-locked for nearly 9500 years. Furthermore, the Chandler wobble—a subtle oscillation in Earth's rotational axis—has been shown to contain harmonic signatures linked to the Jovian planets [59].

Given the scope and diversity of the available literature, a comprehensive review of all proposed mechanisms by which planetary motions might influence solar dynamics is beyond the limits of this section. It is also acknowledged that not all studies carry the same evidentiary weight; some may reflect speculative correlations or statistical coincidences. Nonetheless, common physical objections—such as the argument that planetary bodies are too distant to exert meaningful influence on solar processes—have been addressed in multiple publications [7, 8, 14, 22–25, 36]. Taken together, the cumulative evidence offers a compelling case for the planetary-synchronized solar dynamo hypothesis, which merits continued investigation and serious scientific consideration.

3. Evidence of Interannual and Multidecadal Planetary Cycles in Global Surface Temperature Records

Robust evidence in favor of a planetary contribution to climate variability arises from the identification of multiple astronomical cycle signatures—ranging from interannual to multidecadal scales—within global surface temperature datasets covering the period 1850–2020 [15, 29]. Figures 7A and 7B illustrate a time-frequency comparison between the Sun's velocity relative to the solar system's barycenter and the HadCRUT3 global temperature record [60]. Spectral coherence analysis shows that temperature data reveal oscillatory patterns that align with several planetary cycles operating on decadal and multidecadal timescales.

The spectral decomposition of the solar motion reveals distinct peaks at 5.93, 6.62, 7.42, 9.93, 11.86, 13.8, 20, and 60 years—most of which correspond to the orbital interactions of Jupiter and Saturn. Temperature records exhibit similar periodicities, with peaks near 5.93, 6.62, 7.42, 9.1, 10.4, 13.8, 20, and 60 years. While the 9.1- and 10.4-year cycles are not directly attributable to the Jupiter–Saturn system, they are nonetheless physically interpretable. The 9.1-year signal may reflect a combination between the 8.85-year lunar apsidal precession, the 9.0-year harmonic of the Saros eclipse cycle, and the 9.3-year harmonic of the soli-lunar nodal cycle [52, 61–63]. The 10.4-year cycle falls within the sunspot activity band and likely represents a thermal response to the solar cycle, which has varied in duration from longer phases around 1900 to shorter ones near 2000.

These periodicities form the foundation of the semi-empirical climate model developed in Ref. [29]. The model integrates two components: one based on oscillations derived from astronomical harmonics, and another accounting for anthropogenic and volcanic forcings. The astronomical module includes cycles at 9.1, 10.5, 20, and 60 years, along with longer-term modulations at approximately 115 and 1000 years. The millennial-scale oscillation is not strictly sinusoidal, as it is modulated by the 2318-year Hallstatt cycle. Consequently, the model predicts peaks near 1080 and 2060, and a pronounced minimum around 1700, which coincides with the Maunder Minimum. The phase structure of this millennial cycle is derived from the Jupiter–Saturn harmonic model illustrated in Figures 4 and 5.

The harmonic component of the proposed semiempirical climate model is then expressed as

$$H(t) = \sum_{i=1}^{13} A_i sin[2\pi f_i \cdot (t - 2000) + 2\pi q_i]. \quad (11)$$

Table 4. Parameters of the harmonic component of the astronomical-climate model used for Equation (11) and Equation (12). (Adapted from Ref. [8].)

Cycle i	A_i Â °C	f_i 1/year	T_i year	ϕ_i 1/year
1	0.3228	0.001316	760	0.171
2	0.0584	0.008696	115	0.424
3	0.0858	0.01639	61	0.152
4	0.0334	0.0500	20	0.148
5	0.0241	0.09615	10.4	0.020
6	0.0265	0.1075	9.3	0.497
7	0.0216	0.1340	7.46	0.711
8	0.0272	0.1666	6.00	0.617
9	0.0260	0.1912	5.23	0.409
10	0.0326	0.2088	4.79	0.931
11	0.0276	0.2754	3.63	0.767
12	0.0254	0.2809	3.56	0.792
13	0.0247	0.3484	2.87	0.975

The frequencies, amplitudes, and phases of the chosen 13 harmonics are listed in Table 4. The frequencies and phases are derived from astronomical and solar data, while the amplitudes are estimated from climatic data.

The anthropogenic (*ant*) plus volcanic (*vol*) component was estimated by halving the ensemble mean of the CMIP6 global climate models (GCM) simulations. Thus, the full semi-empirical proposed climate model is written as

$$T(t) = H(t) + f_{ant+vol}(t) \approx H(t) + 0.5 \cdot T_{GCM}(t), \quad (12)$$

where $T_{GCM}(t)$ represents the GCM ensemble average simulation from 1850 to 2100, which changes assuming different emission scenarios for the 21st century which depend on each specific "*Shared Socioeconomic Pathway*" (SSP).

This modelling allows for a rather accurate reproduction of the natural climatic oscillations observed in the instrumental record and suggests that such internal variability could explain up to half the warming recorded between 1970 and 2000. In contrast, CMIP6 general circulation models (GCMs) attribute the entire warming to the anthropogenic forcing alone [12]. A key limitation of these models lies in their minimal representation of solar forcing, which makes the solar contribution nearly negligible in their simulations. However, satellite data from the ACRIM composite indicate a long-term increase in total solar irradiance (TSI) during that period, pointing to a more significant solar role in the observed warming [16, 64]. This upward trend in solar activity between 1970 and 2000 is also predicted by the planetary-based solar model illustrated in Figures 2A and 4C.

Figure 7C presents the ensemble mean outputs of the CMIP6 GCMs, based on historical forcings from 1850 to 2014 and extended to 2100 using projected anthropogenic emissions under three shared socioeconomic pathway (SSP) scenarios [65]. These simulations are compared to the HadCRUT3, HadCRUT4, and HadCRUT5 global temperature datasets [60, 66, 67].

Figure 7D compares the same temperature records with the outputs of the semi-empirical model described by Equation (12).

A direct comparison between Figures 7C and 7D reveals that the semi-empirical model offers a substantially more accurate reconstruction of observed global surface temperatures from 1850 to 2020. Moreover, its projections for future warming under the same SSP scenarios are clearly more moderate than those produced by the CMIP6 GCM ensemble because of the reduced climate sensitivity to radiative forcing relative to that of the GCM [12, 17].

4. Conclusion

The empirical evidences summarized above offer strong support to the hypothesis that solar activity is influenced by planetary dynamics across a wide range of temporal scales—from monthly fluctuations to millennial cycles. In fact, the timing and duration of solar oscillations can be correlated with the periodicities and the phases of planetary harmonics. Similar cycles are also present in terrestrial climate archives, pointing to a broader dynamical coherence between solar and climatic systems. The results suggest that both solar variability and climate changes may be governed, at least in part, by the harmonic architecture of the solar system itself. Coherent oscillations are found with the $M \geq 7$ earthquake historical worldwide record and volcanic activity [68, 69], which suggests an even more general link between planetary-solar cycles and climate-solid Earth activity.

Among the most frequently documented solar cycles are those with durations of approximately 0.3–0.33 years, 1.05–1.15 years, 10–12 years (Schwabe cycle), 20–24 years (Hale cycle), 40–45 years, 55–65 years, 80–105 years (Gleissberg cycle), 115–150 years, 170–190 years (Jose cycle), 200–240 years (Suess–de

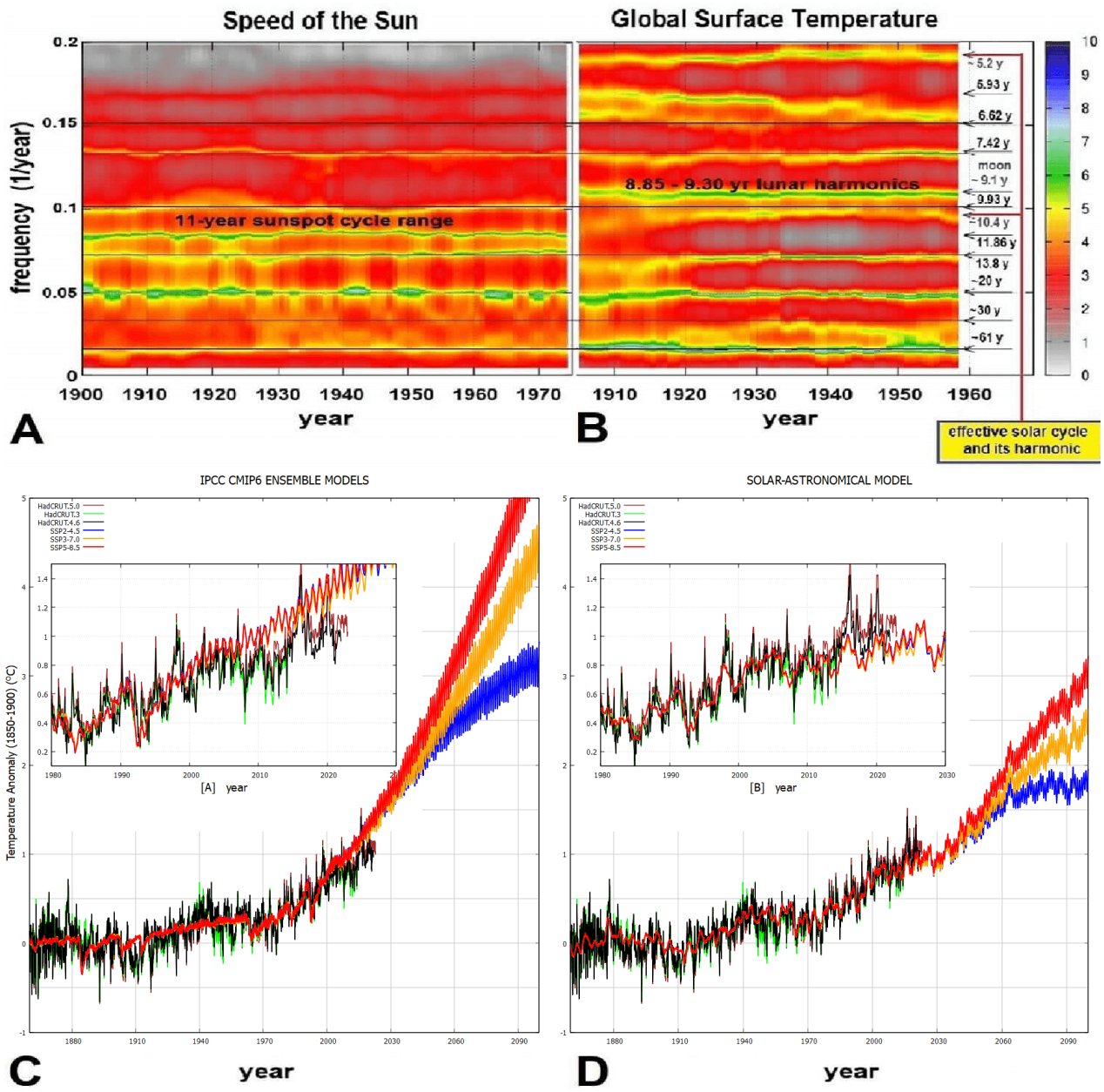

Figure 7. (**A**) Time-frequency analysis (window length $L = 110$ years) of the Sun's velocity relative to the solar system's barycenter. (**B**) Time-frequency analysis ($L = 110$ years) of the detrended HadCRUT3 global temperature dataset [15]. (**C**) Comparison between HadCRUT3, HadCRUT4, and HadCRUT5 temperature records [57,63,64] and CMIP6 GCM ensemble simulations under three SSP scenarios. (**D**) Comparison of the same temperature records with the solar–astronomical harmonic climate model (Equation (12)) [29]. (From Ref. [8].)

Vries cycles), 800–1200 years (Eddy cycle), and 2000–2500 years (Bray–Hallstatt cycle). The spectral correlation between these solar cycles and those of the clusters of the planetary invariant inequality harmonics—as derived from orbital periods, synodic interactions, and spring tidal effects—questions the models that attribute solar variability solely to internal dynamo processes.

Although the exact physical mechanisms behind the planetary synchronization of solar activity remain under investigation, the empirical correlations are consistent and statistically significant. Gravitational tidal interactions may play a role, especially if internal solar dynamics amplify their influence [14, 70]. Additional mechanisms may also be involved. For example, some specific planetary alignments of the Jovian planets could modulate the magnetic structure of the whole solar system, thereby affecting the space weather around Earth through the modulation of the influx of cosmic rays, interstellar particles, and solar wind [7, 8, 37]. Some other specific climate oscillations, such as the approximately 9-year cycle, could be triggered by long-scale soli-lunar tidal forcings.

Given the extensive body of these evidences, we recommend continued exploration of these phenomena. Finally, we emphasize the importance of taking into account also natural climate oscillations, as discussed in Section 3. For instance, Figure 7D shows that under the moderate SSP2-4.5 emission scenario, global mean surface temperatures by 2100 would remain below 2 °C above pre-industrial levels (1850–1900). This result aligns with the goals of the Paris Agreement without requiring the stringent Net-Zero policies embedded in the SSP1 scenarios [12, 17].

Author Contributions

N.S.: Writing – review & editing, Writing – original draft, Software, Methodology, Investigation, Geophysical Data curation, Formal analysis. A.B: Writing – review & editing.

Funding

This work was supported by any funding.

Institutional Review Board Statement

Not applicable.

Informed Consent Statement

Not applicable.

Data Availability Statement

- Orbital data of the planets: https://nssdc.gsfc.nasa.gov/planetary/factsheet/;
- Sunspot number record: https://www.sidc.be/silso/datafiles
- 9400-year solar activity reconstruction (Steinhilber et al., 2012): https://www.ncei.noaa.gov/access/paleo-search/study/12894
- The $\Delta^{14}C$ record (Reimer et al., 2004, IntCal04.14c): https://www.radiocarbon.org/IntCal04.htm

Declaration of Competing Interest

The authors declare that they have no known competing financial interests or personal relationships that could have appeared to influence the work reported in this paper. Co-author Nicola Scafetta is an Editorial Board Member of this Journal and was not involved in the editorial review or the decision to publish this article.

Use of AI and AI-Assisted Technologies

No AI tools were utilized for this paper.

References

1. Eddy, J.A. Climate and the changing Sun. *Clim. Change* **1977**, *1*, 173–190. https://doi.org/10.1007/BF01884410
2. Wolf, R. Extract of a letter to Mr. Carrington. *Mon. Not. R. Astron. Soc.* **1859**, *19*, 85–86. https://doi.org/10.1093/mnras/19.3.85
3. Malburet, J. Sur la période des maxima d'activité solaire. *Acad. Sci. Paris.* Republished in *C. R. Geosci.* **2019**, *351*, 351–354. https://doi.org/10.1016/j.crte.2019.04.001
4. Malburet, J. Sur la cause de la périodicité des taches solaires. *L'Astronomie* **1925**, *39*, 503. https://gallica.bnf.fr/ark:/12148/bpt6k9628963x/f369.item
5. Wood, K. Physical sciences: Sunspots and planets. *Nature* **1972**, *240*, 91–93. https://doi.org/10.1038/240091a0
6. Charbonneau, P. The planetary hypothesis revived. *Nature* **2013**, *493*, 613–614. https://doi.org/10.1038/493613a
7. Scafetta, N.; Bianchini, A. The planetary theory of solar activity variability: A review. *Front. Astron. Space Sci.* **2022**, *9*, 937930. https://doi.org/10.3389/fspas.2022.937930
8. Scafetta, N.; Bianchini, A. Overview of the spectral coherence between planetary resonances and solar and climate oscillations. *Climate* **2023**, *11*, 77. https://doi.org/10.3390/cli11040077
9. Neff, U.; Burns, S.J.; Mangini, A.; et al. Strong coherence between solar variability and the monsoon in Oman between 9 and 6 kyr ago. *Nature* **2001**, *411*, 290–293. https://doi.org/10.1038/35077048
10. Kirkby, J. Cosmic rays and climate. *Surv. Geophys.* **2007**, *28*, 333–375. https://doi.org/10.1007/s10712-008-9030-6
11. Scafetta, N. Multi-scale harmonic model for solar and climate cyclical variation throughout the Holocene based on Jupiter-Saturn tidal frequencies plus the 11-year solar dynamo cycle. *J. Atmos. Sol.-Terr. Phys.* **2012**, *80*, 296–311. https://doi.org/10.1016/j.jastp.2012.02.016
12. Scafetta, N. Detection, attribution, and modeling of climate change: Key open issues. *Gondwana Res.* **2025**. https://doi.org/10.1016/j.gr.2025.05.001
13. Steinhilber, F.; Abreu, J.A.; Beer, J.; et al. 9,400 years of cosmic radiation and solar activity from ice cores and tree rings. *Proc. Natl. Acad. Sci. USA* **2012**, *109*, 5967–5971. https://doi.org/10.1073/pnas.1118965109
14. Scafetta, N. Does the Sun work as a nuclear fusion amplifier of planetary tidal forcing? A proposal for a physical mechanism based on the mass-luminosity relation. *J. Atmos. Sol.-Terr. Phys.* **2012**, *81–82*, 27–40. https://doi.org/10.1016/j.jastp.2012.04.002
15. Scafetta, N. Discussion on the spectral coherence between planetary, solar and climate oscillations: A reply to some critiques. *Astrophys. Space Sci.* **2014**, *354*, 275–299. https://doi.org/10.1007/s10509-014-2111-8
16. Scafetta, N. Empirical assessment of the role of the Sun in climate change using balanced multi-proxy solar records. *Geosci. Front.* **2023**, *14*, 101650. https://doi.org/10.1016/j.gsf.2023.101650
17. Scafetta, N. Impacts and risks of "realistic" global warming projections for the 21st century. *Geosci. Front.* **2024**, *15*, 101774. https://doi.org/10.1016/j.gsf.2023.101774
18. Bendandi, R. *Un principio fondamentale dell'Universo*; Osservatorio Bendandi: Faenza, Italy, 1931. See also http://daltonsminima.altervista.org/2011/01/10/il-ciclo-undecennale-del-sole-secondo-bendandi/
19. Hung, C.-C. Apparent relations between solar activity and solar tides caused by the planets, NASA Tech. Memo. TM-2007-214817, 2007. Available at: http://ntrs.nasa.gov/search.jsp?R=20070025111
20. Wilson, I.R.G. The Venus-Earth-Jupiter spin-orbit coupling model. *Pattern Recogn. Phys.* **2013**, *1*, 147–158. https://doi.org/10.5194/prp-1-147-2013

21. Tattersall, R. The Hum: Lognormal distribution of planetary-solar resonance. *Pattern Recogn. Phys.* **2013**, *1*, 185–198. https://doi.org/10.5194/prp-1-185-2013
22. Stefani, F.; Giesecke, A.; Weber, N.; et al. Synchronized helicity oscillations: A link between planetary tides and the solar cycle? *Sol. Phys.* **2016**, *291*, 2197–2212. https://doi.org/10.1007/s11207-016-0968-0
23. Stefani, F.; Giesecke, A.; Weber, N.; et al. On the synchronizability of Tayler-Spruit and Babcock-Leighton type dynamos. *Sol. Phys.* **2018**, *293*, 12. https://doi.org/10.1007/s11207-017-1232-y
24. Stefani, F.; Giesecke, A.; Weier, T. A model of a tidally synchronized solar dynamo. *Sol. Phys.* **2019**, *294*, 60. https://doi.org/10.1007/s11207-019-1447-1
25. Stefani, F.; Horstmann, G.M.; Klevs, M.; et al. Rieger, Schwabe, Suess-de Vries: The sunny beats of resonance. *Sol. Phys.* **2024**, *299*, 51. https://doi.org/10.1007/s11207-024-02295-x
26. Okhlopkov, V.P. 11-Year index of linear configurations of Venus, Earth, and Jupiter and solar activity. *Geomagn. Aeron.* **2020**, *60*, 381–390. https://doi.org/10.1134/S0016793220030147
27. Scafetta, N. Solar oscillations and the orbital invariant inequalities of the solar system. *Sol. Phys.* **2020**, *295*, 33. https://doi.org/10.1007/s11207-020-01599-y
28. Scafetta, N.; Milani, F. Spectral structure of the solar inertial motion from 12999 BC to 16998 AD. *Publ. Astron. Soc. Pac.* **2025**, *137*, 054402. https://doi.org/10.1088/1538-3873/add37a
29. Scafetta, N. Reconstruction of the interannual to millennial scale patterns of the global surface temperature. *Atmosphere* **2021**, *12*, 147. https://doi.org/10.3390/atmos12010147
30. Tan, B.; Cheng, Z. The mid-term and long-term solar quasiperiodic cycles and the possible relationship with planetary motions. *Astrophys. Space Sci.* **2013**, *343*, 511–521. https://doi.org/10.1007/s10509-012-1272-6
31. Ogurtsov, M.G.; Nagovitsyn, Y.A.; Kocharov, G.E.; et al. Long-period cycles of the Sun's activity recorded in direct solar data and proxies. *Sol. Phys.* **2002**, *211*, 371–394. https://doi.org/10.1023/a:1022411209257
32. Steinhilber, F.; Beer, J.; Frohlich, C. Total solar irradiance during the Holocene. *Geophys. Res. Lett.* **2009**, *36*, L19704. https://doi.org/10.1029/2009GL040142
33. McCracken, K.G. Beer, J.; Steinhilber, F.; et al. A phenomenological study of the cosmic ray variations over the past 9400 years, and their implications regarding solar activity and the solar dynamo. *Sol. Phys.* **2013**, *286*, 609–627. https://doi.org/10.1007/s11207-013-0265-0
34. McCracken, K.G.; Beer, J.; Steinhilber, F. Evidence for planetary forcing of the cosmic ray intensity and solar activity throughout the past 9400 years. *Sol. Phys.* **2014**, *289*, 3207–3229. https://doi.org/10.1007/s11207-014-0510-1
35. Charvátová, I. Can origin of the 2400-year cycle of solar activity be caused by solar inertial motion? *Ann. Geophys.* **2000**, *18*, 399–405. https://doi.org/10.1007/s00585-000-0399-x
36. Abreu, J.A.; Beer, J.; Ferriz-Mas, A.; et al. Is there a planetary influence on solar activity? *Astron. Astrophys.* **2012**, *548*, A88. https://doi.org/10.1051/0004-6361/201219997
37. Scafetta, N.; Milani, F.; Bianchini, A.; et al. On the astronomical origin of the Hallstatt oscillation found in radiocarbon and climate records throughout the Holocene. *Earth-Sci. Rev.* **2016**, *162*, 24–43. https://doi.org/10.1016/j.earscirev.2016.09.004
38. Kutschera, W.; Patzelt, G.; Steier, P.; et al. The Tyrolean Iceman and his glacial environment during the Holocene. *Radiocarbon* **2017**, *59*, 395–405. https://doi.org/10.1017/RDC.2016.70
39. Alley, R.B.; et al. GISP2 Ice Core Temperature and Accumulation Data. In *IGBP PAGES/World Data Center for Paleoclimatology Data Contribution Series #2004-013*; NOAA/NGDC Paleoclimatology Program: Boulder, CO, USA, 2004. https://www.ncei.noaa.gov/access/paleo-search/study/6080
40. Cauquoin, A.; Raisbeck, G.M.; Jouzel, J.; et al. No evidence for planetary influence on solar activity 330,000 years ago. *Astron. Astrophys.* **2014**, *561*, A132. https://doi.org/10.1051/0004-6361/201322879
41. Smythe, C.M.; Eddy, J.A. Planetary tides during Maunder sunspot. *Nature* **1977**, *266*, 434–435. https://doi.org/10.1038/266434a0
42. Poluianov, S.; Usoskin, I. Critical analysis of a hypothesis of the planetary tidal influence on solar activity. *Sol. Phys.* **2014**, *289*, 2333–2342. https://doi.org/10.1007/s11207-014-0475-0
43. Abreu, J.A.; Albert, C.; Beer, J.; et al. Response to: "Critical Analysis of a Hypothesis of the Planetary Tidal Influence on Solar Activity". *Sol. Phys.* **2014**, *289*, 2343–2344. https://doi.org/10.1007/s11207-014-0473-2
44. Bard, E.; Raisbeck, G.; Yiou, F.; et al. Solar irradiance during the last 1200 years based on cosmogenic nuclides. *Tellus B* **2000**, *52*, 985–992. https://doi.org/10.1034/j.1600-0889.2000.d01-7.x
45. Ljungqvist, F.C. A new reconstruction of temperature variability in the extra-tropical Northern Hemisphere during the last two millennia. *Geogr. Ann. Ser. A Phys. Geogr.* **2010**, *92*, 339–351. https://doi.org/10.1111/j.1468-0459.2010.00399.x
46. Moberg, A.; Sonechkin, D.M.; Holmgren, K.; et al. Highly variable Northern Hemisphere temperatures reconstructed from low- and high-resolution proxy data. *Nature* **2005**, *433*, 613–617. https://doi.org/10.1038/nature03265
47. Reimer, P.J.; Baillie, M.G.L.; Bard, E.; et al. Intcal04 terrestrial radiocarbon age calibration, 0–26 cal kyr BP. *Radiocarbon* **2004**, *46*, 1029–1058. https://doi.org/10.1017/S0033822200032999
48. Usoskin, I.; Gallet, Y.; Lopes, F.; et al. Solar activity during the Holocene: The Hallstatt cycle and its consequence for grand minima and maxima. *Astron. Astrophys.* **2016**, *587*, A150. https://doi.org/10.1051/0004-6361/201527295
49. Bray, J. Glaciation and solar activity since the Fifth Century BC and the solar cycle. *Nature* **1968**, *220*, 672–674. https://doi.org/10.1038/220672a0
50. Vasiliev, S.S.; Dergachev, V.A. The 2400-year cycle in atmospheric radiocarbon concentration: Bispectrum of 14C data over the last 8000 years. *Ann. Geophys.* **2002**, *20*, 115–120. https://doi.org/10.5194/angeo-20-115-2002
51. Charvátová, I. Can origin of the 2400-year cycle of solar activity be caused by solar inertial motion? *Ann. Geophys.* **2000**, *18*, 399–405. https://doi.org/10.1007/s00585-000-0399-x
52. Cionco, R.G.; Pavlov, D.A. Solar barycentric dynamics from a new solar-planetary ephemeris. *Astron. Astrophys.* **2018**, *615*, A153. https://doi.org/10.1051/0004-6361/201732349
53. Fairbridge, R.W.; Shirley, J.H. Prolonged minima and the 179-yr cycle of the solar inertial motion. *Sol. Phys.* **1987**, *110*, 191–210. https://doi.org/10.1007/BF00148211
54. Bertolucci, S.; Zioutas, K.; Hofmann, S.; et al. The Sun and its planets as detectors for invisible matter. *Phys. Dark Univ.* **2017**, *17*, 13. https://doi.org/10.1016/j.dark.2017.06.001
55. Petrakou, E. Planetary statistics and forecasting for solar flares. *Adv. Space Res.* **2021**, *68*, 2963–2973. https://doi.org/10.1016/j.asr.2021.05.034
56. Scafetta, N.; Willson, R.C. Planetary harmonics in the historical Hungarian aurora record (1523–1960). *Planet. Space Sci.* **2013**, *78*, 38–44. https://doi.org/10.1016/j.pss.2013.01.005
57. Sharp, G.J. Are Uranus & Neptune responsible for solar grand minima and solar cycle modulation? *Int. J. Astron. Astrophys.* **2013**, *3*, 260–273. https://doi.org/10.4236/ijaa.2013.33031
58. Abreu, J.A.; Beer, J.; Ferriz-Mas, A.; et al. Is there a planetary influence on solar activity? *Astron. Astrophys.* **2012**, *548*, A88. https://doi.org/10.1051/0004-6361/201219997
59. Lopes, F.; Le Mouël, J.L.; Courtillot, V.; et al. On the shoulders of Laplace. *Phys. Earth Planet. Inter.* **2021**, *316*, 106693. https://doi.org/10.1016/j.pepi.2021.106693
60. Brohan, P.; Kennedy, J.J.; Harris, I.; et al. Uncertainty estimates in regional and global observed temperature changes: A new dataset from 1850. *J. Geophys. Res.* **2006**, *111*, D12106. https://doi.org/10.1029/2005JD006548

61. Scafetta, N. Empirical evidence for a celestial origin of the climate oscillations and its implications. *J. Atmos. Sol.-Terr. Phys.* **2010**, *72*, 951–970. https://doi.org/10.1016/j.jastp.2010.04.015
62. Keeling, C.D.; Whorf, T.P. The 1,800-year oceanic tidal cycle: A possible cause of rapid climate change. *Proc. Natl. Acad. Sci. USA* **2000**, *97*, 3814–3819. https://doi.org/10.1073/pnas.97.8.3814
63. Wood, K. Physical sciences: Sunspots and planets. *Nature* **1972**, *240*, 91–93. https://doi.org/10.1038/240091a0
64. Connolly, R.; Soon, W.; Connolly, M.; et al. How much has the Sun influenced Northern Hemisphere temperature trends? An ongoing debate. *Res. Astron. Astrophys.* **2021**, *21*, 131. https://doi.org/10.1088/1674-4527/21/6/131
65. Eyring, V.; Bony, S.; Meehl, G.A.; et al. Overview of the Coupled Model Intercomparison Project Phase 6 (CMIP6) experimental design and organization. *Geosci. Model Dev.* **2016**, *9*, 1937–1958. https://doi.org/10.5194/gmd-9-1937-2016
66. Morice, C.P.; Kennedy, J.J.; Rayner, N.A.; et al. Quantifying uncertainties in global and regional temperature change using an ensemble of observational estimates: The HadCRUT4 dataset. *J. Geophys. Res.* **2012**, *117*, D08101. https://doi.org/10.1029/2011JD017187
67. Morice, C.P.; Kennedy, J.J.; Rayner, N.A.; et al. An updated assessment of near-surface temperature change from 1850: The HadCRUT5 data set. *J. Geophys. Res. Atmos.* **2021**, *126*, e2019JD032361. https://doi.org/10.1029/2019JD032361
68. Scafetta, N.; Mazzarella, A. Spectral coherence between climate oscillations and the M $\geq$ 7 earthquake historical worldwide record. *Nat. Hazards* **2015**, *76*, 1807–1829. https://doi.org/10.1007/s11069-014-1571-z
69. Bragato, P.L. Italian seismicity and Vesuvius' eruptions synchronize on a quasi 60-year oscillation. *Earth Space Sci.* **2015**, *2*, 453–467. https://doi.org/10.1002/2014EA000030
70. Wolff, C.L.; Patrone, P.N. A new way that planets can affect the Sun. *Sol. Phys.* **2010**, *266*, 227–246. https://doi.org/10.1007/s11207-010-9628-y